Synergistic effect of strontium-substituted hydroxyapatite and microRNA-21 on improving bone remodeling and osseointegration

Zhen Geng, Xiaogang Wang, Jin Zhao, Zhaoyang Li, Lili Ma, Shengli Zhu, Yanqin Liang, Zhenduo Cui, Hongyan He, Xianjin Yang

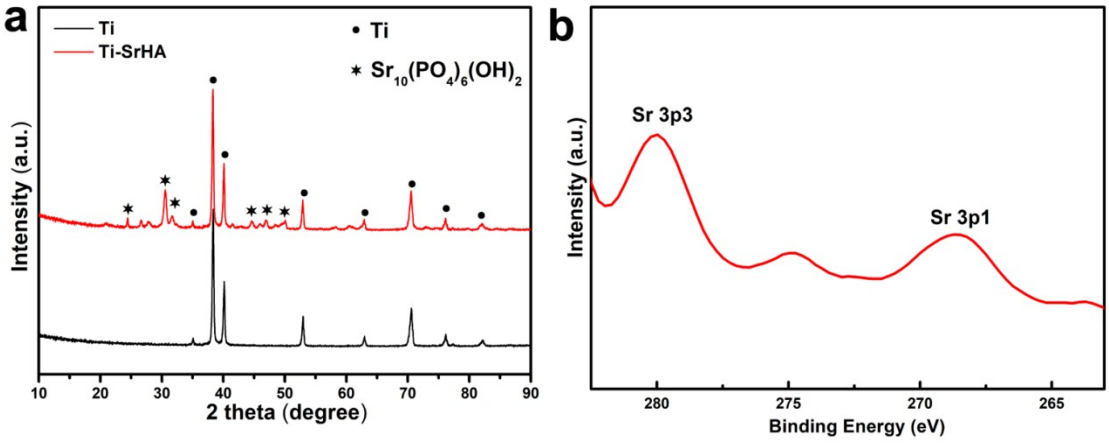

Figure S1 (a) XRD patterns of Ti and Ti-SrHA. (b) High-resolution Sr3p spectra of Ti-SrHA.

The XRD results indicated that the main component of the Ti-SrHA coating is $Sr_{10}(PO_4)_6(OH)_2$ as compared with pure Ti (**Figure S1** a). The high-resolution Sr3p spectra further confirmed the SrHA depositon (**Figure S1** b).

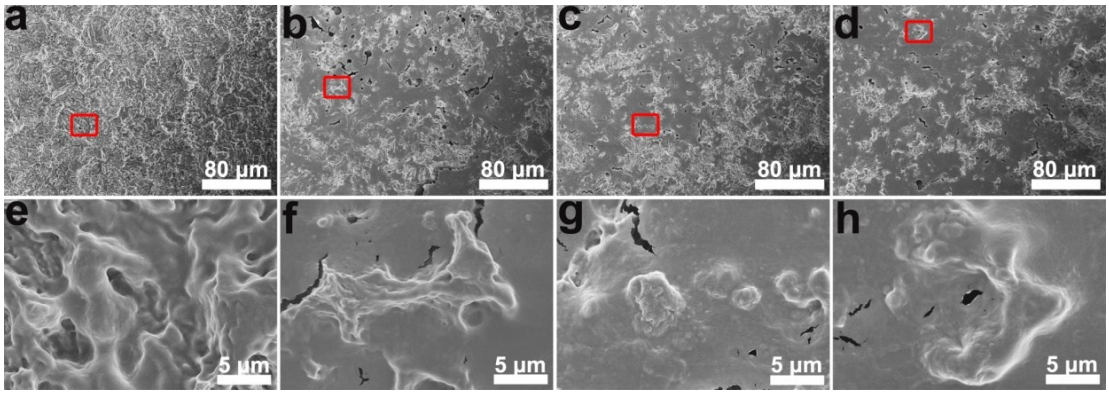

Figure S2 SEM morphologies of MG63 cell after culturing for 14 days.
(a, e) Ti, (b, f) Ti-SrHA, (c, g) Ti-21, (d, h) Ti-SrHA-21.

In order to evaluate the *in vitro* mineralization capacity of each sample, the MG63 cells SEM morphology were observed after 14 days culturing, as shown in **Fig. S2**. It could be seen that the coated groups showed higher cell coverage rate than Ti. In addition, there were more calcium nodules on the coated samples, especially for Ti-SrHA-21. These results indicated SrHA and miR-21 had a synergistic effect on *in vitro* mineralization.

Osteoclastic activity

1. **Cell culture.** We cultured bone marrow mononuclear cells (BMMCs) obtained from six- to eight-week-old C57BL/6 mice. The cells were maintained in α-MEM (Gibco, USA) with 10% FBS, 30 ng/mL M-CSF, 100μg/mL streptomycin and 100 U/mL penicillin.
2. **Osteoclast formation and activity assays.** BMMCs were cultured with M-CSF (30 ng/mL, R&D, USA) and RANKL (50 ng/mL, R&D, USA) to induce osteoclast formation. For TRAP staining, the specimens were gently washed twice with PBS and transferred to a new 12-well plate. Mature osteoclasts were recovered from the specimens using 0.25% trypsin and seeded in new 24-well plates. After allowing the cells to adhere for 2 h, a TRAP staining kit (Sigma-Aldrich, USA) was used to assess osteoclast formation. Cell images were taken with a microscope (Nikon ECLIPSE TE2000-S, Japan), and the cells with at least three nuclei were identified as osteoclasts. We also measured osteoclast activity using a TRAP enzyme assay kit (Sigma-Aldrich, USA) according to the manufacturer's instructions. Briefly, the specimens were gently washed twice with PBS, transferred to a new 24-well plate and lysed with 0.1% Triton X-100. The supernatant solution was collected, and TRAP enzyme activity was analyzed at 405 nm using a colorimetric plate reader.
3. **Immunofluorescence staining assays.** To further evaluate osteoclast formation on the specimens, actin ring formation assays were performed. After culturing for 5 days, cells were fixed with 4% paraformaldehyde in PBS for 15 min. Then, the cells were permeabilized with 0.1% Triton-X 100 in PBS for 5 min. The actin cytoskeleton was stained with phalloidin (USA) 1:100 in PBS for 1 h, and cell nuclei were stained with DAPI (Invitrogen, Carlsbad CA, USA) 1:1,000 in PBS for 15 min. The osteoclast contours and nuclei were visualized under a CLSM (Nikon), and images were captured from five random fields. The areas of F-actin rings were analyzed via the ImageJ software (Bethesda, USA). The percent nuclei in F-actin was expressed as an index for fusion efficiency, which was calculated as nuclei within F-actin rings divided by total nuclei.

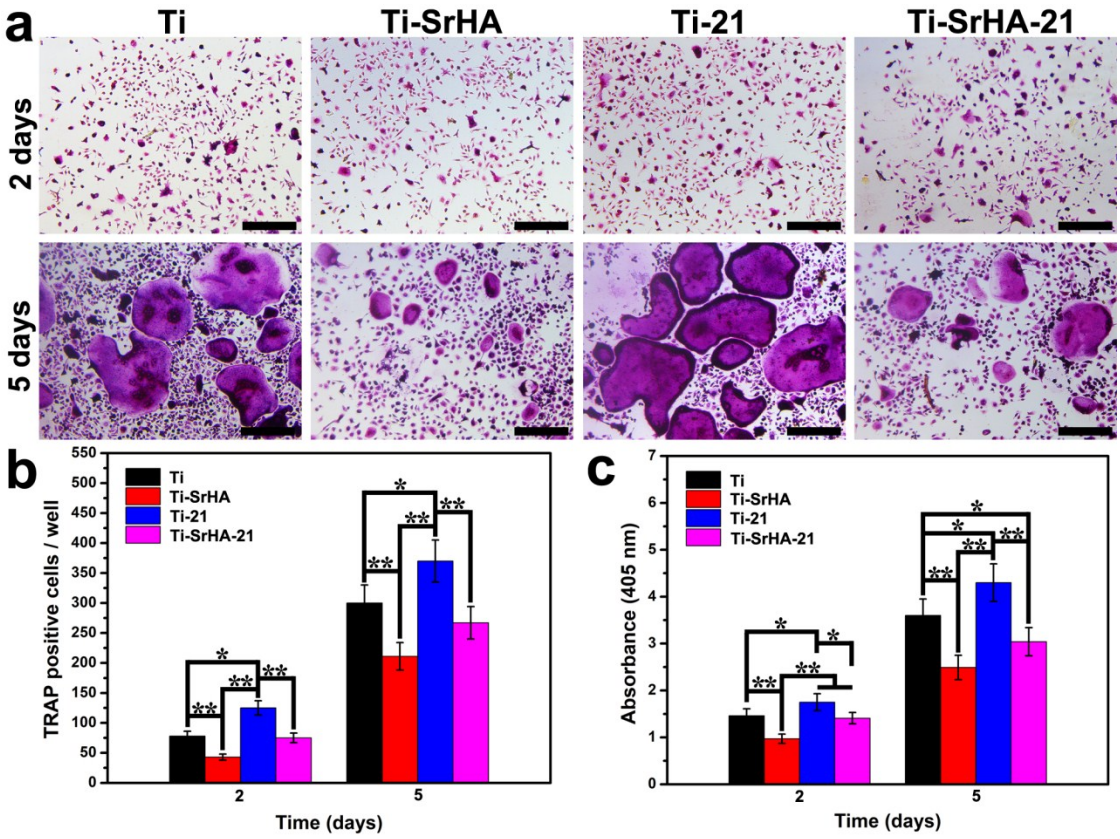

Figure S3 (a) TRAP staining of osteoclasts at each harvest point. Scale bars, 400 μm. (b) Quantification of the cell number of TRAP-positive osteoclasts with greater than 3 nuclei. (c) TRAP enzyme activity was measured at OD 405 nm. Statistically significant differences, $^{*}p < 0.05$, $^{**}p < 0.01$.

The e□ects of the di□erent samples on osteoclast formation were evaluated by TRAP staining. As shown in **Figure S3 a** and **b**, after 2 and 5 days culturing, the TRAP-positive multinuclear cells on the Ti-SrHA and Ti-SrHA-21 groups were less than those on the Ti and Ti-21 groups. Meanwhile, the TRAP activity results showed that the activity of Ti-SrHA and Ti-SrHA-21 were significantly lower than those of Ti and Ti-21 groups (**Figure S3 c**). These findings indicated that SrHA could inhibit osteoclast formation and osteoclastic activity.

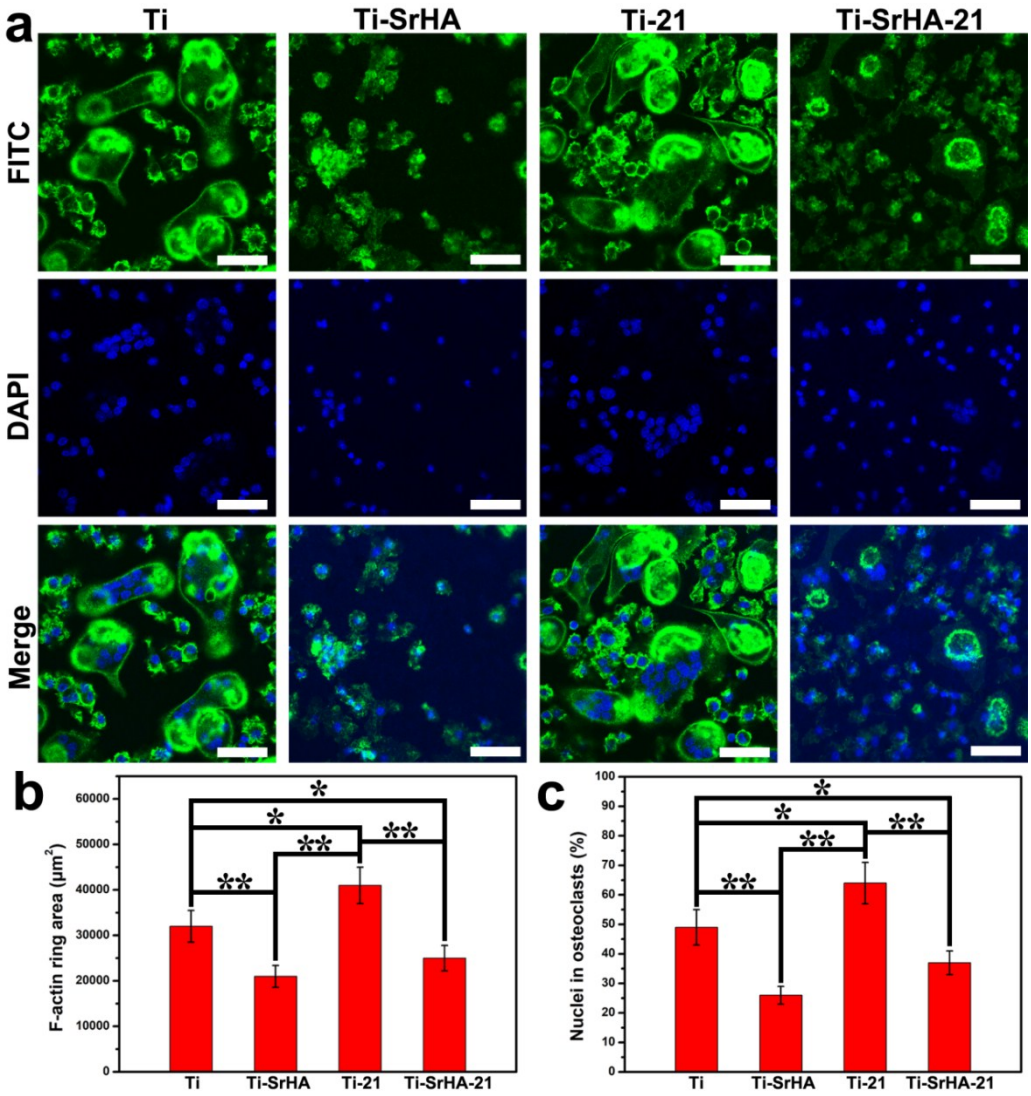

Figure S4 (a) Confocal micrographs of differentiated osteoclasts immunostained for F-actin (green) and cell nuclei (blue). Scale bar = 200 μm. (b) Quantification of the F-actin ring area and (c) % nuclei in osteoclasts. Statistically significant differences, $^{*}p < 0.05$, $^{**}p < 0.01$.

The immunofluorescence staining assay revealed that the formation of actin rings in multinucleated osteoclasts was reduced by SrHA (**Figure S4 a**). The average F-actin ring areas of Ti-SrHA and Ti-SrHA-21 were significantly lower than those of Ti and Ti-21 groups (**Figure S4 b**). In addition, the quantitative results showed that the percentage of nuclei in F-actin rings (fusion efficiency) was significantly lower in the Ti-SrHA and Ti-SrHA-21 groups (**Figure S4 c**).

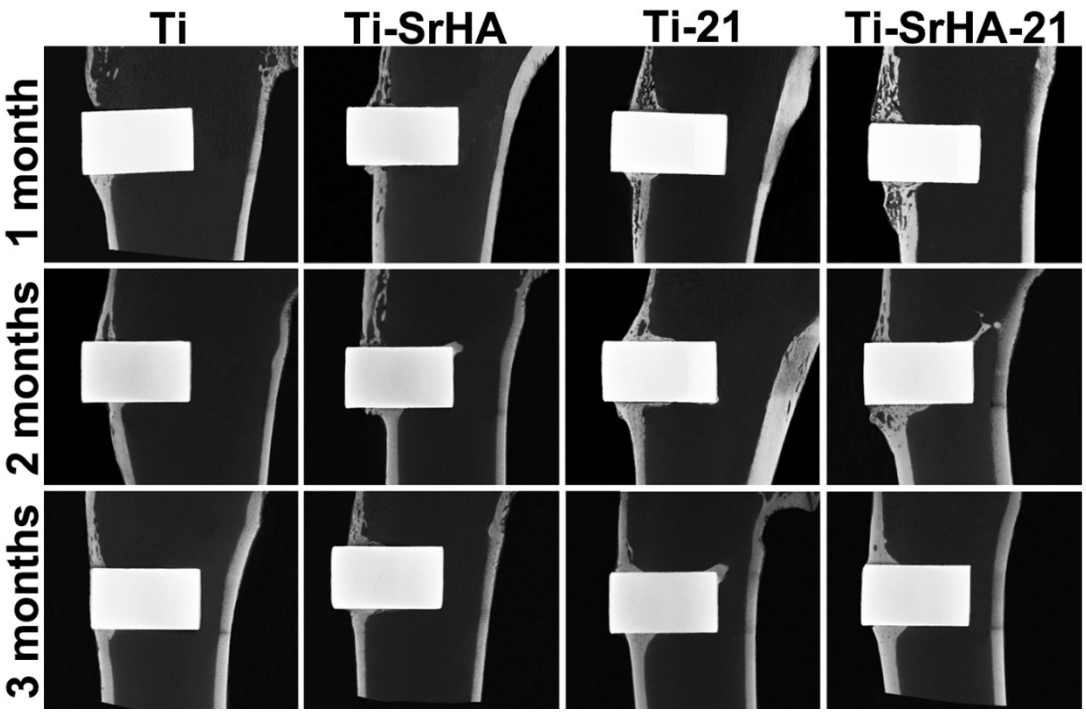

Figure S5 Micro-CT images (cross-section) of the bone-implant boundary.

Micro-CT was used to further evaluate the bone-implant boundary. At 1 month, there were obvious gaps between new bone and all groups, especially for Ti. After implantation for 2 months, there were still obvious gaps existed around Ti and Ti-SrHA groups. Whereas for Ti-21 and Ti-SrHA-21, they not only showed good bonding with new bone but also exhibited remarkable osteoinductivity. After surgery for 3 months, there was no obvious gap between bone and each sample. Meanwhile, Ti-21 and Ti-SrHA-21 exhibited higher bone density and osteoinductivity than Ti and Ti-SrHA, especially for Ti-SrHA-21. These results indicated SrHA and miR-21 had a synergistic effect on osseointegration.

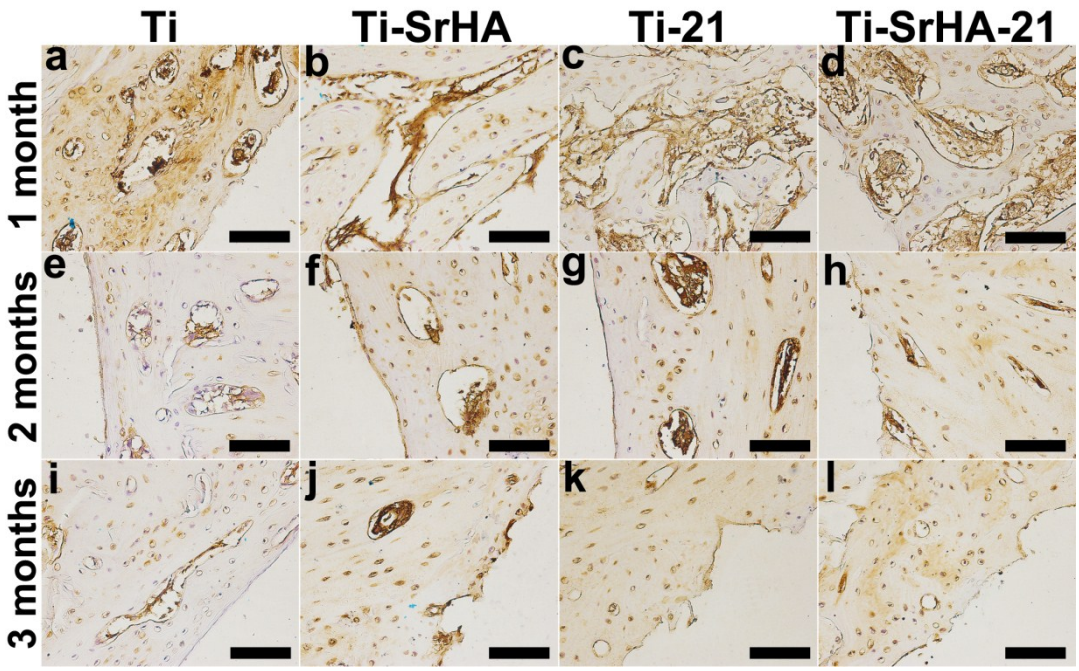

Figure S6 Imunohistochemistry staining of CD31 expression. Scale bars: 100 μm.

CD31 was an important endothelial marker which could contribute to the development of new blood vessels. At 1 month, Ti-21 significantly promoted the expression of CD31. Meanwhile, Ti-SrHA-21 also exhibited high expression of CD. These indicated that miR-21 was beneficial to vascularization. In addition, SrHA could not influence the functions of miR-21.

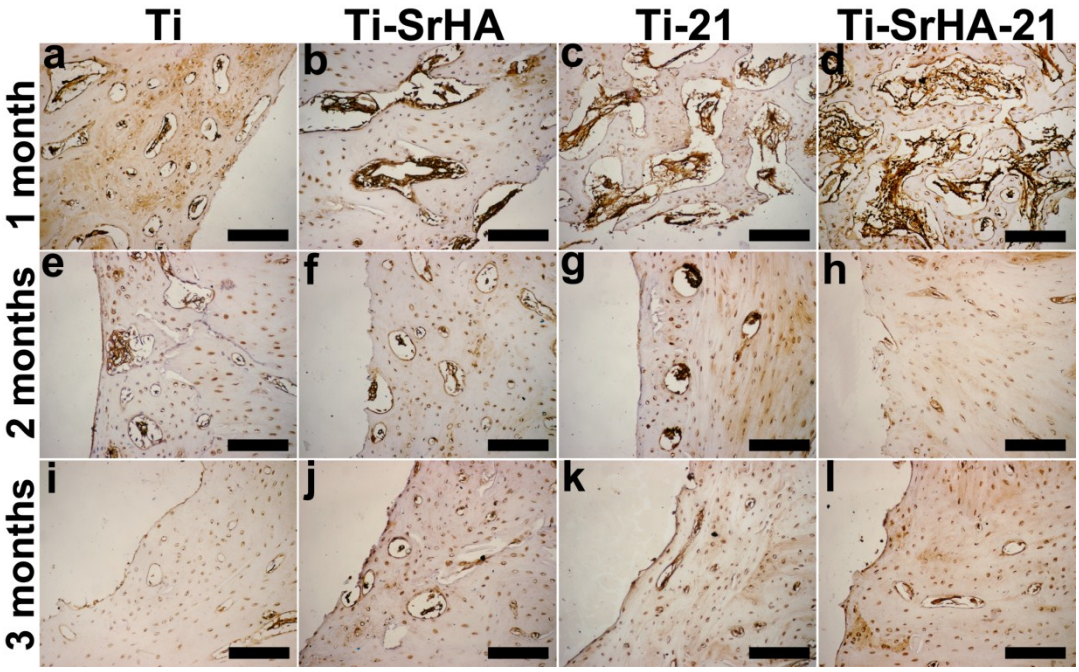

Figure S7 Imunohistochemistry staining of COL-I expression. Scale bars: 100 μm.

Collagen type I (Col-I) acted as a potential structural and adhesion protein, facilitating initial cell adherence. It promoted spreading and proliferation via multiple binding sites, including RGD integrin binding sites, being a signalling protein. After surgery for 1 month, the expression of Col-I was apparently enhanced on the coated groups, especially for Ti-SrHA. After implantation for 2~3 months, Col-I expression was decreased in all groups, which was mainly due to the decreased bone lacunas.

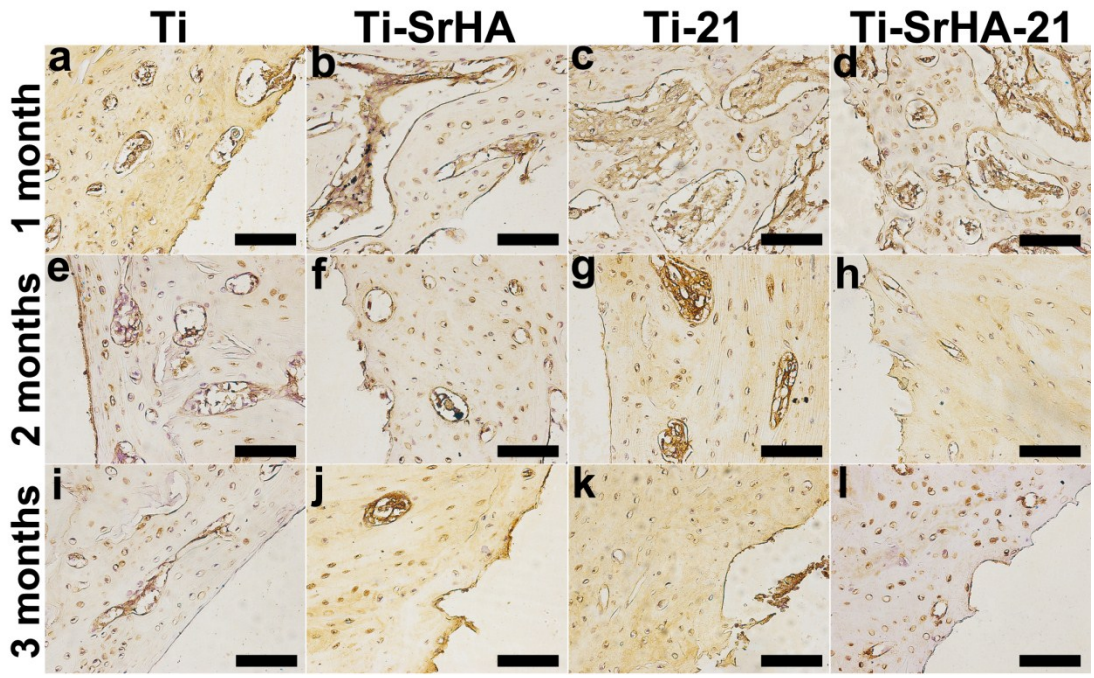

Figure S8 Imunohistochemistry staining of Runx2 expression. Scale bars: 100 μm.

Runx2 was an essential transcription factor that played an essential role in osteoblast differentiation. Forced expression of Runx2 in non-osteoblastic cells induced the expression of osteocalcin, osteopontin, and bone sialoprotein. After 1 month implantation, Ti-SrHA-21 presented obviously improvement of Runx2 expression. As the bone lacunas filled with bone trabecular, Runx2 expression decreased for all groups.

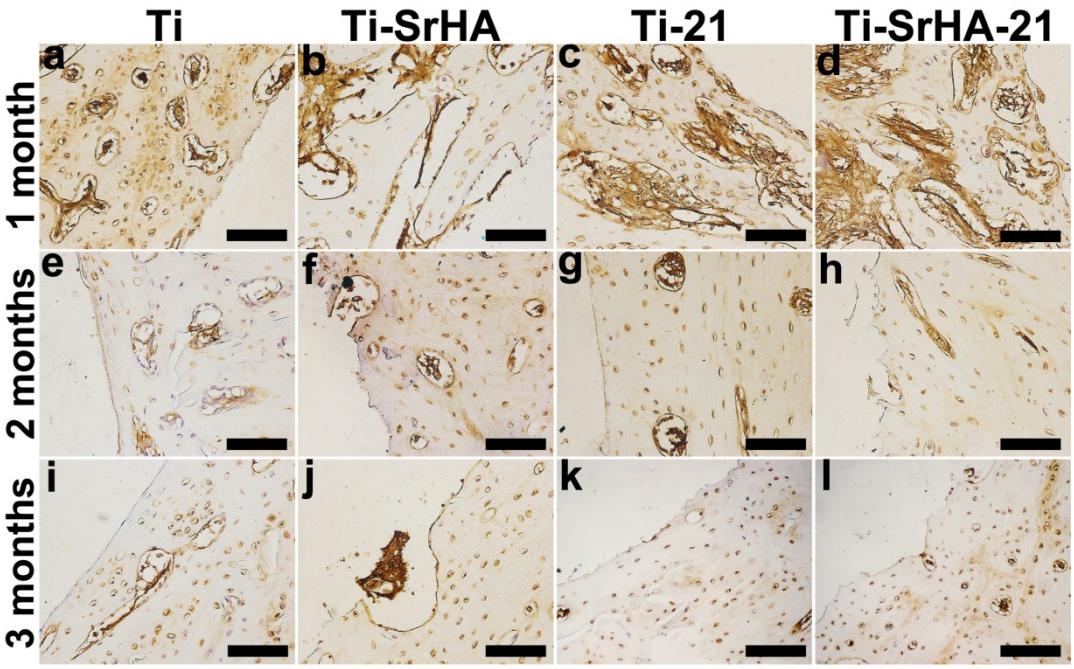

Figure S9 Imunohistochemistry staining of OCN expression. Scale bars: 100 μm.

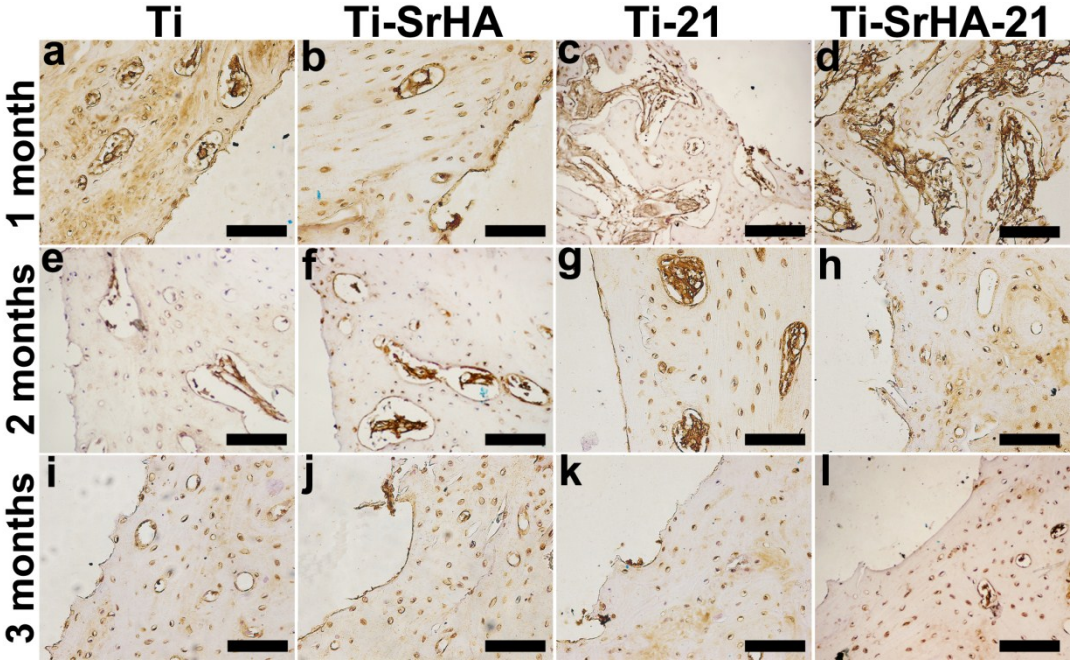

Figure S10 Imunohistochemistry staining of OPN expression. Scale bars: 100 μm.

OCN exerted a mechanical function within the bone matrix. As a result of its ability to tightly bind hydroxyapatite and form a complex with collagen through the matrix protein OPN, OCN was proposed as means to bridge the matrix and mineral fractions of bone tissue. OPN is a highly acidic glycosylated phosphoprotein, which is involved in bone cell attachment to ECM and acts as a chemoattractant for bone cells

during the early stage of bone development. In addition, OPN plays an essential role in adhesion, remodeling, and osseointegration at the interface between a biomaterial and bone. As shown in **Fig. S9~S10**, the coated groups showed enhanced expression of both OCN and OPN at the early stages, especially for Ti-SrHA-21. This indicated that the composite coating was beneficial to bone formation. After 3 months healing, Ti-SrHA-21 still showed higher expression of OCN and OPN than other groups.

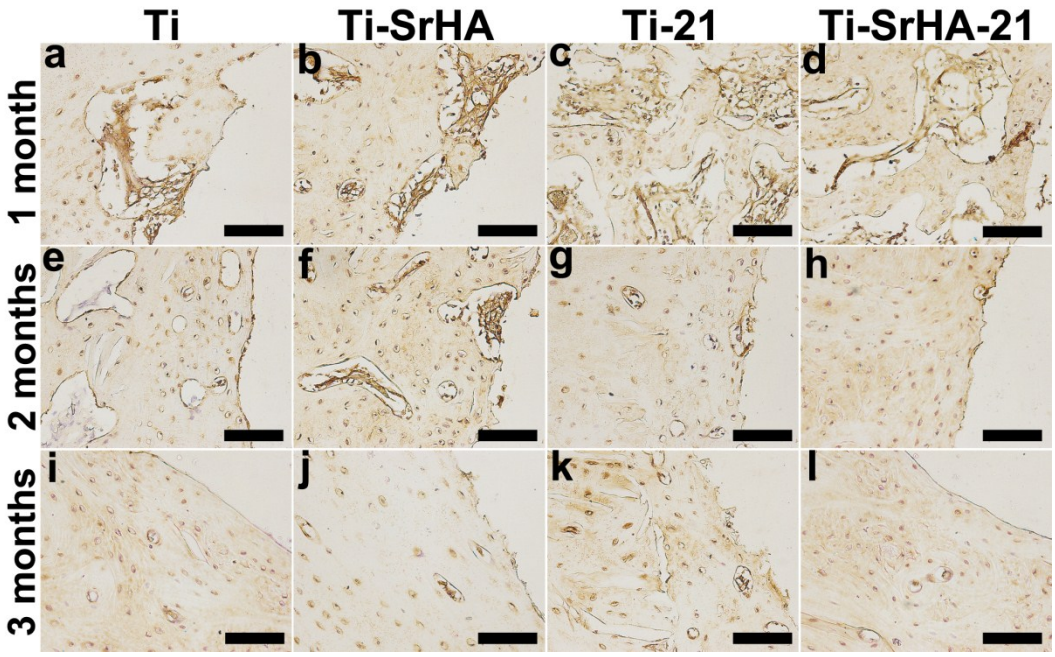

Figure S11 Imunohistochemistry staining of OPG expression. Scale bars: 100 μm.

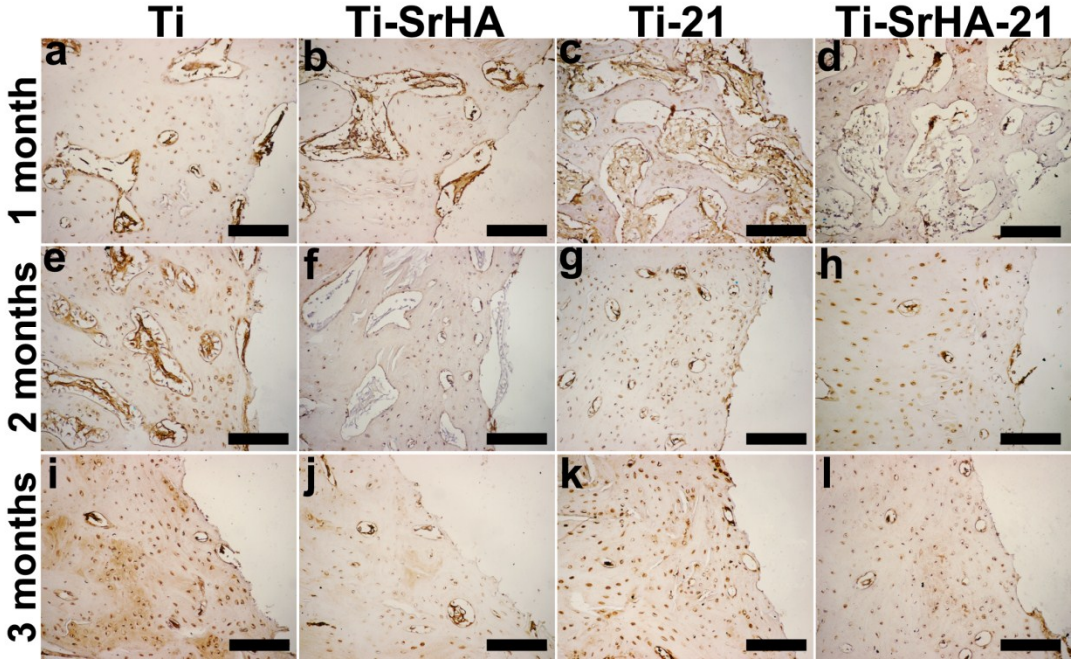

Figure S12 Imunohistochemistry staining of RANKL expression. Scale bars: 100 μm.

OPG and RANKL proteins are mediators of several cell processes, including bone metabolism. OPG could bind to RANKL and inhibited osteoclastogenesis. Thus, the dynamics of bone remodeling could be summarized as OPG leading to bone formation and RANKL leading to bone resorption. As shown in **Fig. S11** and **S12**, the immunohistochemistry results showed that both the expression of OPG and RANKL

were significantly increased on Ti-21 groups, indicating a fast bone remodeling process. Meanwhile, the Ti-SrHA-21 groups showed decreased RANKL expression compared with Ti-21 groups. These demonstrated SrHA and miR-21 had a synergistic effect on promoting bone formation and inhibiting bone resorption

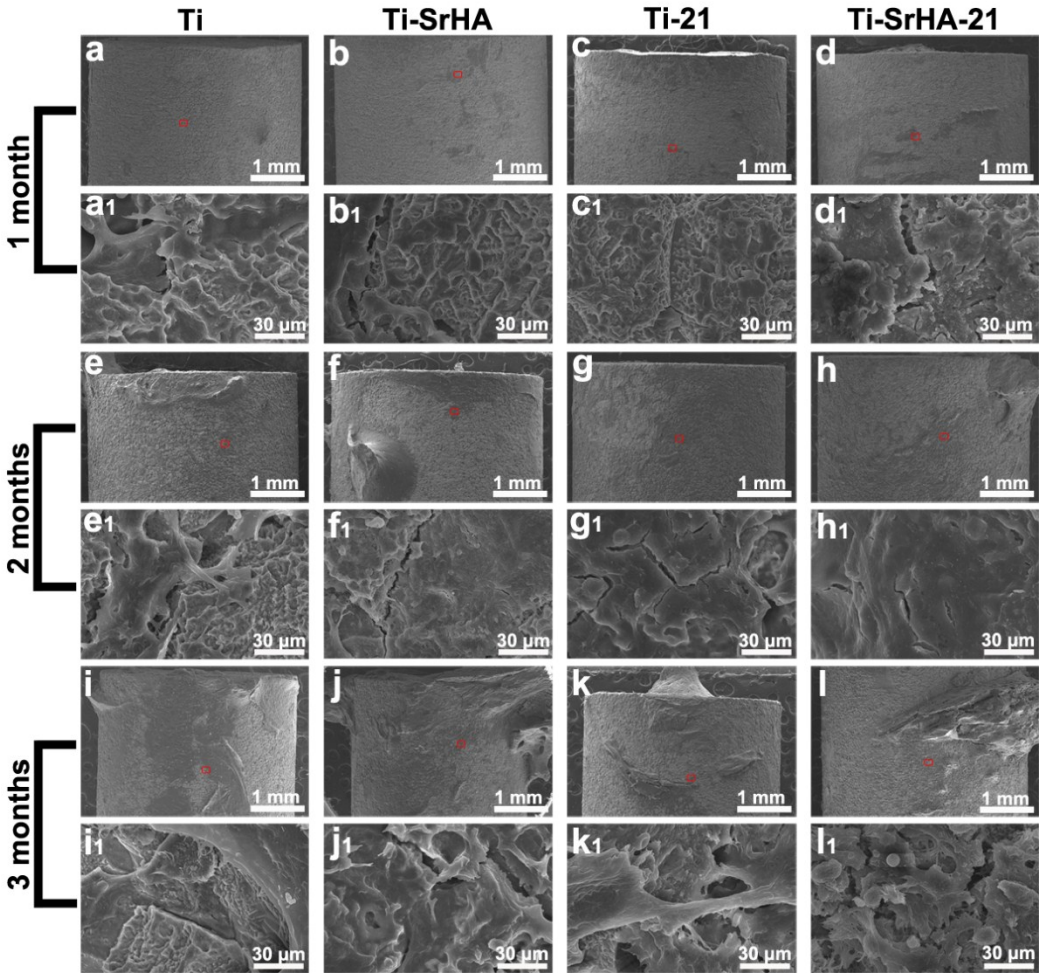

Figure S13 SEM images of the implants surfaces after the implants taken out from the animal body at the indicated time. Pictures with higher magnification are taken from the area enclosed by a square in pictures with lower magnification.

After the biomechanical test, the morphology of the implants surfaces was examined by SEM, as shown in **Figure S13**. At 1 month, there was no obvious bone tissue on the Ti surface. However, there was a small amount of bone tissue on the surfaces of the other three groups (especially for Ti-SrHA-21). After implantation for 2 months, all samples were covered with apparent bone tissue. Meanwhile, it was worth noting that the coated samples (especially for Ti-SrHA-21) exhibited higher bone tissue coverage rate than Ti. After 3 months of healing, there were lots of bone tissues on all samples, indicating increased bone-implant bonding strength. In addition, plenty of nodules were formed on Ti-SrHA and Ti-21. Moreover, a dense structure combined with collagenous fiber and apatite, which was similar to mature bone, was formed on Ti-SrHA-21.